The Various Shape of Nano-Polycrystalline Transparent ZnWO4 Scintillator by Thermal Evaporation Method

Heon Yong Jeong, Ju Hyuk Lee and Sung Oh Cho*

Nuclear and Quantum Eng., KAIST, 291, Daehak-ro, Yuseong-gu, Daejeon, Republic of Korea
*Corresponding author: socho@kaist.ac.kr

1. Introduction

High-resolution X-ray imaging is promising applications in field of X-ray micro-radiography of biology, archeology, materials and non-destructive test. [1-3] The spatial resolution is the one of the most important parameters in high-resolution X-ray imaging. [4] It is affected by the thickness of a scintillator because the optical detector with small effective pixel size is highly sensitive to the light spread phenomenon. [5] To minimize the light spread phenomenon, many researchers have tried to fabricated several micrometers thin-layer scintillators for high-resolution X-ray imaging.

In this study, the transparent thin-film scintillator composed of nano-polycrystalline zinc tungstate ($ZnWO_4$) was fabricated on quartz glass using thermal evaporation method with sintering. $ZnWO_4$ has been used for a long time as an X-ray scintillator because the crystallized $ZnWO_4$ has 2.3 times more luminescence characteristics than $Bi_4Ge_3O_{12}$ (BGO) under X-ray irradiation [6] In addition, It is high density (ρ = 7.87 g/cm^3), high effective atomic number. (Z_{eff} = 61)[7,8] Since $ZnWO_4$ has high X-ray absorption capability relative to ρZ^4_{eff}, it has the potential to be utilized in thin-film scintillators. There have been a growing body of research to fabricate transparent ceramic thin-films using the thermal evaporation method with sintering. [9] The thermal evaporation method is the efficient approach to facilely deposit the thin and uniform film on complex structure. The main purpose of this study is to demonstrate that nano-polycrystalline $ZnWO_4$ thin-film scintillator can be applied to the high-resolution X-ray imaging. In addition, This method can fabricate various shapes of thin-film scintillators, showing the possibility that it can be used in various fields of high-resolution X-ray imaging.

2. Methods and Results

2.1 Fabrication of $ZnWO_4$ Thin Film

Zinc oxide and tungsten oxide nanoparticles were purchased from Sigma-Aldrich (St. Louis, MO, USA). These nanoparticles were added to ethanol with a 1:1 atomic ratio between zinc and tungsten. The solutions were mixed through the vibrating ball milling and dried in air at 60 °C. The resulting powders were heated in an electric furnace at 1000 °C for 5 h to induce the solid-state reaction.

$ZnWO_4$ powders fabricated by the solid-state reaction were used as the source material in thermal evaporation method. Tungsten boat was used as evaporating crucible. The deposition on quartz glass (B&C Tech, Daejeon, South Korea) was carried out at about 10^{-6} Torr. The holder is rotated 25 cm away from the crucible. After deposition, the bare $ZnWO_4$ thin-films were sintered in air furnace at 600, 700, 800 and 900 °C for 3 hour.

2.2 Fabrication of $ZnWO_4$ Thin Film

Figure 1a shows the photographs of 3 μm $ZnWO_4$ thin-film sintered at 600, 700, 800 and 900 °C and photographs in 254 nm UV irradiation. Figure 1b shows the XRD patterns of these films. These XRD patterns show that these films were crystallized into pure monoclinic $ZnWO_4$. Figure 1c shows the spectra of transmission rate in wavelength from 200 nm to 800 nm. The most transparent samples were the films sintered at 600 and 700 °C and the transmission rate were 81% and 78% respectively at 480 nm wavelength. The $ZnWO_4$ thin-films sintered at 800 and 900 °C had transmission rate of 68% and 56% at 480 nm wavelength respectively.

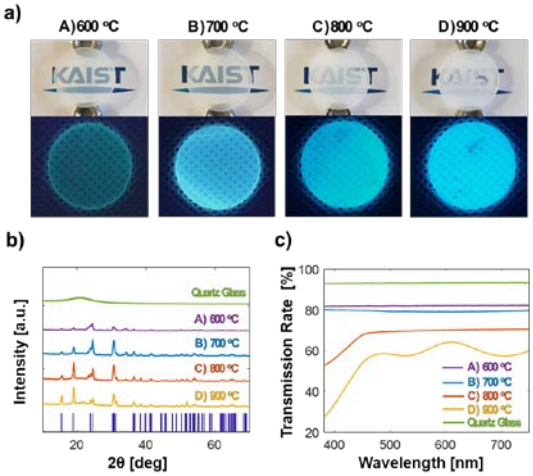

Figure 1. a) Photographs of $ZnWO_4$ thin-film sintered at A) 600, B) 700, C) 800 and D) 900 °C and in 265 nm UV irradiation, b) XRD spectra, c) Transmission rate spectra of $ZnWO_4$ thin-film sintered at A) 600, B) 700, C) 800, D) 900 °C and bare quartz glass

The structure morphologies of $ZnWO_4$ thin-films sintered at different temperatures are showed in Figure 2 by FE-SEM. After sintering, the amorphous film becomes a crystallized film. In the case of $ZnWO_4$ thin-film sintered at 900 °C, many pores and cracks in the

wavelength scale of optical light were formed. (Figure 2d) These pores and cracks reduce transparency. In other words, when it is used as a scintillator, the optical light scattering occurs, resulting in a problem of reducing spatial resolution of X-ray image. The $ZnWO_4$ thin-films sintered at 600, 700 and 800 °C are composed of polycrystalline structures. The grain sizes were measured through FE-SEM to use the intercept technique. The average grain sizes sintered at 600, 700 and 800 °C were 92.6, 157.3 and 698.7 nm.

The difference of transmission rate can be explained by Mie scattering theory. When the grain size is comparable to the wavelength of optical light, Mie scattering occurs at grain boundaries. However, when the grain size is sufficiently smaller than the wavelength of optical light, Mie scattering is suppressed to allow the optical light to penetrate the film. Therefore, $ZnWO_4$ thin-films sintered at 600 and 700 °C with the grains smaller than the optical wavelength were the most transparent.

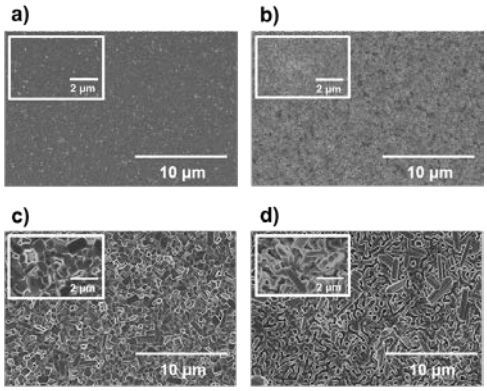

Figure 2. SEM images of $ZnWO_4$ thin-film sintered at a) 600, b) 700, c) 800 and d) 900 °C

The sintered $ZnWO_4$ thin-films were irradiated by X-ray and UV to evaluate the luminescent properties. (Figure 3) When the sintering temperatures were 700, 800, and 900 °C, a relatively high intensity of light emission was measured without a significant difference because the amorphous films were completely crystallized. The emission intensity of the $ZnWO_4$ thin-film sintered at 600 °C was lower than 700 °C or more because the amorphous film did not completely change into crystallized structure (Figure 3b). Although the $ZnWO_4$ thin-film sintered at 600 °C has the best transparency, it is impossible to utilized as a scintillator.

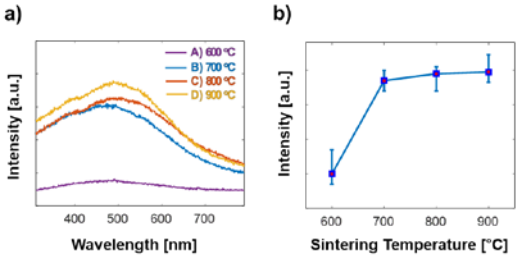

Figure 3. a) PL spectra in 325 nm UV irradiation and b) the emission intensities in X-ray irradiation of $ZnWO_4$ thin-film scintillator sintered at 600, 700, 800 and 900 °C (Error bars represent standard deviation of 20 independent measurements).

In the case of sintering at 800 °C, the emission intensity was increased by about 3.7% compared to the case of sintering at 700°C. However, since the film sintered at 700 °C has smaller grains size, the optical light scattering occurs less. The spatial resolution which is an important factor of high-resolution X-ray images is increased. (Figure 4) As a result, the film sintered at 700°C is the most optimized film which the average grain size is 157.3 nm.

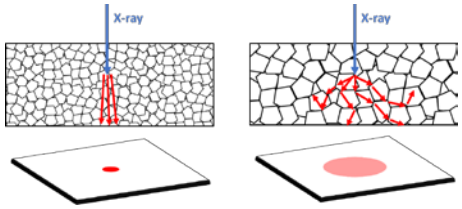

Figure 4. The effect of grain size of polycrystalline film scintillator in high-resolution X-ray imaging

2.3 Evaluation of X-ray Imaging Performance

The nanoparticle screen scintillator was manufactured and the spatial resolution was compared in high resolution X-ray imaging system. The $ZnWO_4$ nanoparticles screen scintillator was fabricated using solid-state reaction and drop-casting method, and the particle size was similar to the grain size of the optimized nano-polycrystalline $ZnWO_4$ film. The structure of the nano-polycrystalline film and nanoparticle screen is shown in figure 5. In the case of a nanoparticle screen, the particles are separated from each other and there is a air-gap. The optical light generated from the scintillator is scattered due to the difference of refractive index between the particles and air-gap. In the case of a nano-polycrystalline film, there is no gap because the nano-grains are closely packed. There is no difference in refractive index at the grain boundary, so optical light scattering can be suppressed.

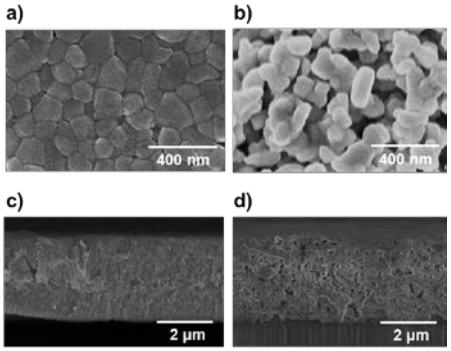

Figure 5. Surface SEM images of a) nano-polycrystalline $ZnWO_4$ film scintillator and b) $ZnWO_4$

nanoparticle screen scintillator. Cross-sectional SEM images of c) nano-polycrystalline $ZnWO_4$ film scintillator and d) $ZnWO_4$ nanoparticle screen scintillator

The schematic of high-resolution X-ray imaging system is shown in Figure 6a. Figure 6b and Figure 6c show the X-ray images of the 1500-mesh transmission electron microscope (TEM) grid obtained from the high-resolution X-ray imaging system. The nano-polycrystalline film shows the better spatial resolution than nanoparticle screen scintillator in high-resolution X-ray imaging. The high-resolution X-ray image of the JIMA RT RC-02 test pattern (JIMA, Chiyodaku, Japan) was developed using a nano-polycrystalline film. (Figure 6d) This image shows that nano-polycrystalline transparent $ZnWO_4$ thin-film scintillator has high performance to resolve 2 μm line and space patterns when it is utilized in high-resolution X-ray imaging.

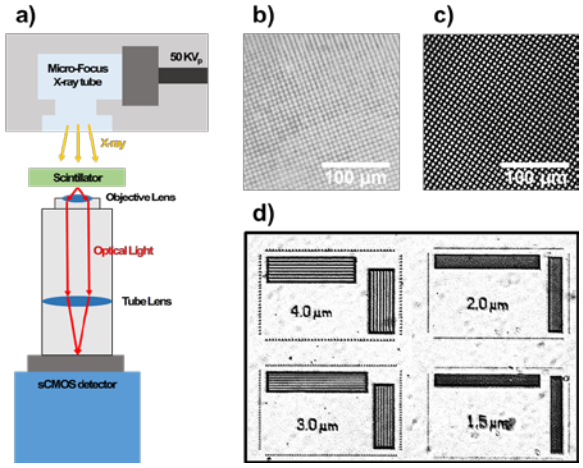

Figure 6. a) Schematic of high-resolution X-ray imaging system, high-Resolution X-ray images of a 1500-mesh TEM grid obtained by b) nanoparticle screen scintillator and c) nano-polycrystalline film scintillator and d) high-resolution X-ray image of JIMA RT RC-02 test pattern developed by nano-polycrystalline film

Thermal evaporation method allows fabrication of the pixelated scintillator as shown in Figure 7a and Figure 7b and the curved scintillator as shown in 7c. The nano-polycrystalline $ZnWO_4$ film scintillator was deposited on quartz substrates according to micro-patterning mask. (Figure 7a) The thickness of pixelated scintillator can be increased by preventing light spread as shown in Figure 7b, thus increasing X-ray sensitivity. Figure 7c shows curved $ZnWO_4$ thin-film scintillator under 254 nm UV irradiation. Curved scintillator has the advantage that it can minimize the distortion at the edge of X-ray image in computed tomography (CT). The curved transparent $ZnWO_4$ thin-film scintillator can be used effectively in mico-CT because it has high spatial resolution of X-ray micro-image without image distortion at the edge.

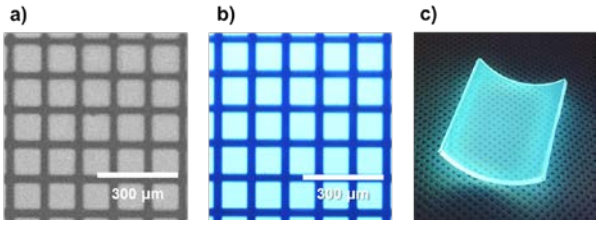

Figure 7. a) SEM image of Different Size of Pixelated Scintillators, b) Optical Microscope Image of Pixelated Scintillators under 254 UV irradiation and c) Curved Scintillator under 254 nm UV irradiation

3. Conclusions

The nano-polycrystalline transparent $ZnWO_4$ thin-film scintillator was fabricated by thermal evaporation method and it was successfully utilized in high-resolution X-ray imaging. Since it has the average grain size of 157.3 nm smaller than optical wavelength, the optical light scattering is suppressed. The optimized 3 μm $ZnWO_4$ thin-film has high optical performance with a transmission rate of 78% at 480 nm wavelength. It was analyzed by high-resolution X-ray imaging system composed of micro-focus X-ray, an optical lens, and sCMOS detector; the effective pixel size is 650 nm. The X-ray image of 2 μm line and space patterns were resolved. In addition, the thermal evaporation method is facile approach to fabricate the various shapes of thin-film scintillators, so it can be used in the various fields of high-resolution X-ray imaging. Nano-polycrystalline transparent $ZnWO_4$ thin-film scintillator is expected to be used effectively in X-ray micro-radiography.

REFERENCES

[1] Mizutani, R.; Suzuki, Y. X-ray microtomography in biology. Micron 2012, 43, 104-115.
[2] Dudak, J.; Zemlicka, J.; Karch, J.; Patzelt, M.; Mrzilkova, J.; Zach, P.; Hermanova, Z.; Kvacek, J.; Krejci, F. High-contrast X-ray micro-radiography and micro-CT of ex-vivo soft tissue murine organs utilizing ethanol fixation and large area photon-counting detector. Scientific reports 2016, 6, 1-9.
[3] Adderley, W.P.; Simpson, I.A.; MacLeod, G.W. Testing high-resolution X-ray computed tomography for the micromorphological analyses of archaeological soils and sediments. Archaeological Prospection 2001, 8, 107-112.
[4] Martin, T.; Koch, A. Recent developments in X-ray imaging with micrometer spatial resolution. Journal of synchrotron radiation 2006, 13, 180-194.
[5] Cha, B.K.; Lee, D.H.; Kim, B.; Seo, C.-W.; Jeon, S.; Huh, Y.; Kim, J.Y.; Cho, G.; Kim, Y. High-resolution X-ray imaging based on pixel-structured CsI: Tl scintillating screens for indirect X-ray image sensors. Journal of the Korean Physical Society 2011, 59, 3670-3673.
[6] Oi, T.; Takagi, K.; Fukazawa, T. Scintillation study of ZnWO4 single crystals. Applied Physics Letters 1980, 36, 278-279.
[7] Ryzhikov, V.; Naydenov, S.; Onyshchenko, G.; Pochet, T.; Smith, C. High efficiency fast neutron detectors based on

inorganic scintillators. In Proceedings of 2014 IEEE Nuclear Science Symposium and Medical Imaging Conference (NSS/MIC); pp. 1-6.
[8] Grassmann, H.; Moser, H.-G.; Lorenz, E. Scintillation properties of ZnWO4. Journal of luminescence 1985, 33, 109-113.
[9] Vaynzof, Y. The future of perovskite photovoltaics—thermal evaporation or solution processing? Advanced Energy Materials 2020, 10, 2003073.